Available online at www.derpharmachemica.com

Scholars Research Library

Der Pharma Chemica, 2015, 7(10):34-44
(http://derpharmachemica.com/archive.html)

ISSN 0975-413X
CODEN (USA): PCHHAX

Electrochemical and gravimetric studies of the corrosion inhibition of mild steel in HCl medium by *cymbopogon nardus* essential oil

K. Alaoui Ismaili[1], S. EL Arouji[1], A. Abdellaoui[2], F. El Kamani [2], Z. Rais[1], M. Filali Baba[1], M. Taleb[1], Khadijah M. Emran[3], A. Zarrouk[4], A. Aouniti[4] and B. Hammouti[4]

[1]Laboratoire d'Ingénierie d'Electrochimie de Modélisation et d'Environnement (LIEME) FSDM Fès, Morocco
[2]Laboratory of Physiology, Pharmacology Health and Environment Unit of Bioremediation and Environment Department of Biology. Faculty of Sciences DM Fès, Morocco
[3]Chemistry Department, Faculty of Science, Taibah University, Saudi Arabia
[4]LCAE-URAC18, Faculty of Science, Mohammed first University, Oujda, Morocco

---

ABSTRACT

Corrosion inhibition effect of cymbopogon nardus essential oil (CNEO) on the mild steel in 1.0 M HCl solution was investigated by electrochemical (potentiodynamic polarization curves, and electrochemical impedance spectroscopy) and weight loss techniques. The corrosion rate of mild steel was decreased in the presence of CNEO. The corrosion inhibition efficiency was found to increase with CNEO concentration to attain 90% with 1.50 g/L at 298 K. The polarization studies showed that CNEO acts as mixed type inhibitor. The effect of temperature on the corrosion rate of mild steel in HCl solution in the absence and presence of CNEO was also studied. Values of corrosion inhibition efficiency calculated from weight loss technique were in good agreement with those obtained from electrochemical techniques. The results showed that the adsorption of the cymbopogon nardus essential oil (CNEO) on the mild steel surface obeys Langmuir isotherm. The activation parameters, apparent activation energy (E_a), the enthalpy of activation (ΔH_a) and entropy of activation (ΔS_a) for the corrosion of mild steel in 1.0 M HCl in the absence and presence of CNEO were calculated and discussed.

INTRODUCTION

Corrosion is a common problem for several metals. In industries, it creates several major problems because of its perilous nature for metals [1]. The damage done by corrosion engenders more costs for the examination, renovation and replacement of various equipment and constitutes serious public and environmental risks. Corrosion of metals cannot be completely stopped, but it can be drastically reduced using various approaches, such as upgrading the materials, blending production fluids, process control and using chemical corrosion inhibitors [2]. Among these methods, the use of chemical corrosion inhibitors is usually the most suitable, practical and economical approach to accomplish this goal [3]. Several synthetic molecules have been reported as valuable corrosion inhibitors for metals [4-25]. However, most of them are expensive and extremely toxic to human being and the environment. The toxicity of synthetic compounds and uncompromising environmental directives have led to the use of natural products as safe and effective green corrosion inhibitors [26,27]. Natural products have the advantage of being biodegradable in nature, renewable, easily accessible, economical and, most importantly, are environmental friendly. Recently, several natural products, particularly plant extracts, have been reported to be an excellent, environmentally benign and economical source of corrosion inhibitors [28,29].

Green inhibitors can be used in the form of extracts, essential oils or pure compounds. Previously, some essential oils have been reported as potential corrosion inhibitors, such as Cedre oil [30], Jojoba oil [31], Artemisia oil [32], Pennyroyal oil [33], Eucalyptus oil [34,35], Lavandula Angustifolia L. oil [36], Verbena oil [37].

Continuing our work on development of green corrosion inhibitors [38-40], the present study investigates the inhibiting effect of *cymbopogon nardus* essential oil (CNEO) on the corrosion of mild steel in HCl solution by weight loss, polarization and electrochemical impedance spectroscopy (EIS) methods.

MATERIALS AND METHODS

Inhibitor

Plant material

Fresh leaves of ***Cymbopogon nardus*** were collected from the Rabat city "Morocco" in the April 2012 and were dried for 7 to 10 days in the shade at room temperature then stored in cloth bags at 5°C and transferred later to the laboratory for preparation of the plant extracts.

Hydrodistillation apparatus and procedure

200g from the air-dried leaves of the ***Cymbopogon nardus*** were subjected to hydrodistillation for 3 h with 600 mL distilled water using a Clevenger-type apparatus according to the European Pharmacopoeia (Fig. 1). The oil obtained was collected and dried over anhydrous sodium sulphate and stored in a refrigerator at 4-5°C prior to analysis. Yield based on dried weight of the sample was calculated [32].

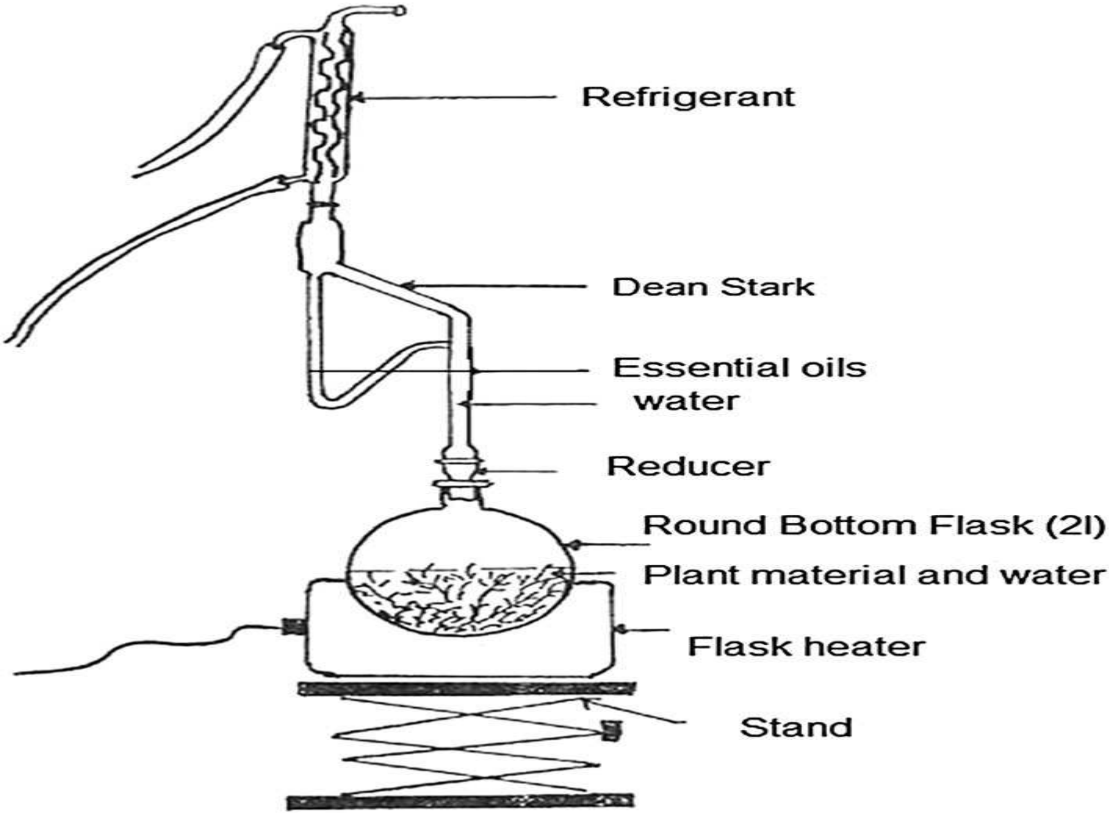

Figure 1: Hydrodistillation of essential oils: Clevenger-type apparatus

Materials

The steel used in this study is a mild steel with a chemical composition (in wt%) of 0.09%P, 0.01 % Al, 0.38 % Si, 0.05 % Mn, 0.21 % C, 0.05 % S and the remainder iron (Fe). The steel samples were pre-treated prior to the experiments by grinding with amery paper sic (220, 400, 800, 1000 and 1200); rinsed with distilled water, degreased in acetone, washed again with bidistilled water and then dried at room temperature before use.

Solutions

The aggressive solutions of 1.0 M HCl were prepared by dilution of analytical grade 37% HCl with distilled water. The test solutions were freshly prepared before each experiment by adding essential oil of *cymbopogon nardus* directly to the corrosive solution. Concentrations of essential oils are 0.15, 0.5, 0.75, 1.0 and 1.5 g/L.

Gravimetric study

Gravimetric experiments were performed according to the standard methods [41], the mild steel sheets of 2 × 1 × 0.2 cm were abraded with a series of emery papers SiC (120, 600 and 1200) and then washed with distilled water and acetone. After weighing accurately, the specimens were immersed in a 50 mL beaker containing 100 mL of 1.0 M HCl solution with and without addition of different concentrations inhibitor. All the aggressive acid solutions were open to air. After 6 h of acid immersion, the specimens were taken out, washed, dried, and weighed accurately. In order to get good reproducibility, all measurements were performed few times and average values were reported to obtain good reproducibility. The inhibition efficiency ($\eta_{WL}\%$) and surface coverage (θ) were calculated as follows:

$$C_{\mathrm{R}} = \frac{W_{\mathrm{b}} - W_{\mathrm{a}}}{At} \quad (1)$$

$$\eta_{\mathrm{WL}}(\%) = \left(1 - \frac{w_{\mathrm{i}}}{w_0}\right) \times 100 \quad (2)$$

$$\theta = \left(1 - \frac{w_{\mathrm{i}}}{w_0}\right) \quad (3)$$

where W_{b} and W_{a} are the specimen weight before and after immersion in the tested solution, w_0 and w_{i} are the values of corrosion weight losses of mild steel in uninhibited and inhibited solutions, respectively, A the total area of the mild steel specimen (cm^2) and t is the exposure time (h).

Electrochemical measurements

The electrochemical measurements were carried out using Volta lab (Tacussel- Radiometer PGZ 100) potentiostate and controlled by Tacussel corrosion analysis software model (Voltamaster 4) at under static condition. The corrosion cell used had three electrodes. The reference electrode was a saturated calomel electrode (SCE). A platinum electrode was used as auxiliary electrode of surface area of 1 cm^2. The working electrode was mild steel of the surface 1 cm^2. All potentials given in this study were referred to this reference electrode. The working electrode was immersed in test solution for 30 min to a establish steady state open circuit potential (E_{ocp}). After measuring the E_{ocp}, the electrochemical measurements were performed. All electrochemical tests have been performed in aerated solutions at 298 K. The EIS experiments were conducted in the frequency range with high limit of 100 kHz and different low limit 0.1 Hz at open circuit potential, with 10 points per decade, at the rest potential, after 60 min of acid immersion, by applying 10 mV ac voltage peak-to-peak. Nyquist plots were made from these experiments. The best semicircle can be fit through the data points in the Nyquist plot using a non-linear least square fit so as to give the intersections with the *x*-axis.

The inhibition efficiency of the inhibitor was calculated from the charge transfer resistance values using the following equation:

$$\eta_z\% = \frac{R^i_{ct} - R^\circ_{ct}}{R^i_{ct}} \times 100 \quad (4)$$

Where, R°_{ct} and $R^{\mathrm{i}}_{\mathrm{ct}}$ are the charge transfer resistance in absence and in presence of inhibitor, respectively.

After ac impedance test, the potentiodynamic polarization measurements of mild steel substrate in inhibited and uninhibited solution were scanned from cathodic to the anodic direction, with a scan rate of 1 mV s^{-1}. The potentiodynamic data were analysed using the polarization VoltaMaster 4 software. The linear Tafel segments of anodic and cathodic curves were extrapolated to corrosion potential to obtain corrosion current densities (I_{corr}).
The inhibition efficiency was evaluated from the measured I_{corr} values using the following relationship:

$$\eta_{\mathrm{Tafel}}(\%) = \frac{I_{\mathrm{corr}} - I_{\mathrm{corr(i)}}}{I_{\mathrm{corr}}} \times 100 \quad (5)$$

where I_{corr} and $I_{\mathrm{corr(i)}}$ are the corrosion current densities for steel electrode in the uninhibited and inhibited solutions, respectively.

RESULTS AND DISCUSSION

Weight Loss Measurements

Weight loss of mild steel surface in 1.0 M HCl was determined at 298, 308, 318, 323 and 333 K in the absence and presence of different concentration of CNEO. The obtained corrosion parameters are depicted in Table 1.

It is clear from the table that the percentage inhibition efficiency increases with concentration (C) of the extract and decreases with temperature. The decrease in corrosion rate (C_R) with increase in concentration of CNEO is due to the fact that the surface coverage of metal increases by the adsorption of inhibitor molecules [42]. The increase in corrosion rate with increase in temperature may be probably due to increased rate of desorption of inhibitor molecules of CNEO from the mild steel surface at higher temperature [43].

Effect of Temperature

Temperature has more pronounced effect on the rate of electrochemical corrosion of metal. In acid medium, C_R increases exponentially with increase in temperature. Also, the decrease of hydrogen overpotential observed at higher temperature [44]. Usually corrosion reactions are regarded as Arrhenius processes and the C_R can be expressed by the relation [45]

$$C_R = A\exp\left(-\frac{E_a}{RT}\right) \qquad (6)$$

where C_R is the corrosion rate, E_a is the apparent activation energy of the mild steel dissolution, R is the molar gas constant, T is the absolute temperature, and A is the frequency factor. Arrhenius plots of Ln C_R versus 1/T for mild steel corrosion in 1.0 M HCl in the absence and presence of different concentration of CNEO are presented in Figure 2, and the calculated parameters are given in Table 2.

Table 1: Corrosion parameters of mild steel in 1.0 M HCl solution in the presence and absence of CNEO at different temperature, obtained from weight loss measurements

	Temperature									
	298 K		308 K		318 K		323 K		333 K	
C (g/L)	C_R (mg/cm^2 h)	η_{WL} (%)	C_R (mg/cm^2 h)	η_{WL} (%)	C_R (mg/cm^2 h)	η_{WL} (%)	C_R (mg/cm^2 h)	η_{WL} (%)	C_R (mg/cm^2 h)	η_{WL} (%)
Blank	0.554	—	0.85	—	1.99	—	2.67	—	5.52	—
1.50	0.05	90.0	0.10	88.2	0.24	87.9	0.58	78.2	1.4	74.6
1.00	0.07	85.2	0.11	87.0	0.27	86.4	0.72	73.0	1.64	70.2
0.75	0.08	82.4	0.12	85.8	0.31	84.4	0.74	72.2	1.72	68.8
0.50	0.09	81.5	0.15	82.3	0.35	83.4	0.79	70.4	1.82	67.0
0.15	0.10	81.3	0.19	77.6	0.47	76.3	0.86	67.7	2.00	63.7

The increase in activation energy after the addition of the inhibitor to the 1.0 M HCl solution indicated that physical adsorption (electrostatic) occurs in the first stage [46]. It can also be concluded that the whole process is controlled by surface reaction since the energy of activation of the corrosion process in the absence and presence of CNEO are greaterthan 20 kJ mol^{-1} [47,48]. Further both the E_a and frequency factor values for inhibited solutions increase with inhibitor concentration which indicates that the addition of CNEO decrease the metal dissolution in 1.0 M HCl by increasing the energy barrier for the corrosion reaction by the adsorption of active organic molecules at the metal surface [49-51].

Table 2: Activation parameters for mild steel corrosion in 1.0 M HCl in the absence and presence of different concentrations of CNEO

Inhibitor	C (g/L)	A (mg/cm^2 h)	E_a (KJ/mol)	ΔH_a (KJ/mol)	ΔS_a (J/(mol K))
	0.00	2.495×10^{9}	55.39	52.77	-73.78
	1.50	4.858×10^{12}	80.27	77.65	-10.81
CNEO	1.00	2.005×10^{12}	77.46	74.85	-18.17
	0.75	1.001×10^{12}	75.41	72.80	-23.94
	0.50	4.388×10^{11}	72.94	70.33	-30.80
	0.15	3.545×10^{11}	71.96	69.34	-32.83

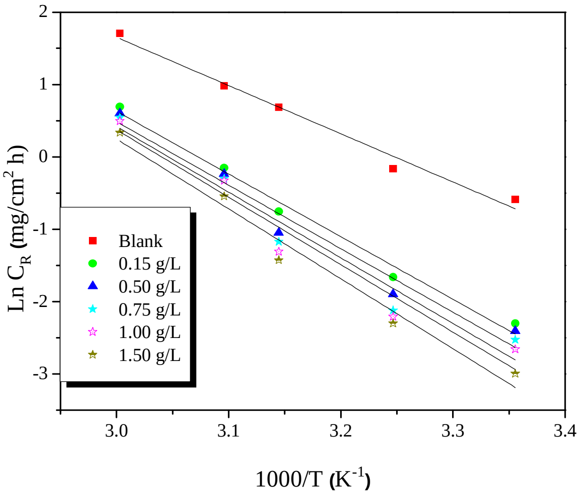

Figure 2: Arrhenius plot for mild steel in 1.0 M HCl in the absence and presence of different concentrations of CNEO

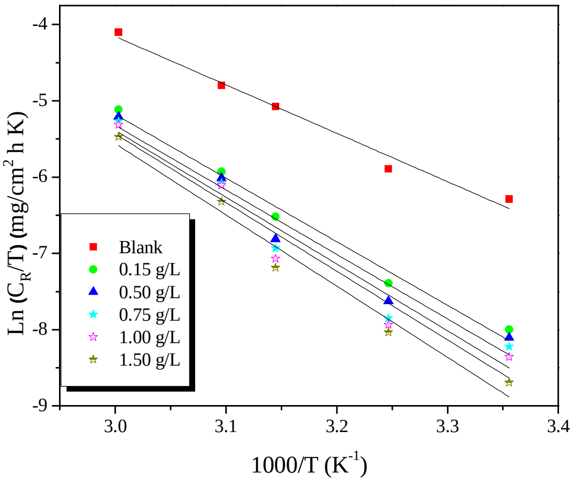

Figure 3: Transition state plot for mild steel in 1.0 M HCl in the absence and presence of different concentrations of CNEO

Further insight into the adsorption mechanism is offered by considering the thermodynamic functions for the mild steel dissolution in 1.0 M HCl in the absence and presence of different concentrations of CNEO. In this regards, Transition state equation was used to evaluate the corrosion activation parameters, namely, the enthalpy of activation (ΔH_a) and entropy of activation (ΔS_a). Transition state equation is given by the expression [52]

$$C_R = \frac{RT}{Nh}\exp\left(\frac{\Delta S_a}{R}\right)\exp\left(-\frac{\Delta H_a}{RT}\right) \qquad (7)$$

where h is Plank's constant, N is Avogrado's number, ΔS_a is the entropy of activation and ΔH_a is the enthalpy of activation.

Figure 3 shows a plot of Ln(C_R/T) vs 1/T. Straight lines were obtained with a slope equal to ($-\Delta H_a/R$) and the intercept was equal to [Ln(R/Nh) + ($\Delta S_a/R$)], from which the values of ΔH_a and ΔS_a were calculated and listed in Table 2. It is evident from the table that the activation parameters (ΔH_a and ΔS_a) of mild steel dissolution reaction in 1.0 M HCl in the presence of CNEO are higher than in the absence of extract. The positive sign of enthalpies reflects the endothermic nature of mild steel dissolution process [53]. Whereas the large and negative values of entropy of activation in the absence and presence of CNEO implies that the rate-determining step for the activated complex is an association step rather than a dissociation step, meaning that during adsorption process the decrease in disordering takes place on moving from reactants to the activated complex [54]. Thus orderliness increases as reactants are converted to activated complex.

Adsorption isotherm

Adsorption isotherms are very important in determining the mechanism of organo-electrochemical reaction [55]. Hence in order to gain more information about the mode of adsorption of CNEO on mild steel surface in 1.0 M HCl at 303, 313, 323, and 333 K, attempts were made to fit experimental data with several adsorption isotherms like Langmuir, Temkin, Freundlich, Bockris-Swinkles, and Flory-Huggins isotherms. However the best fit was obtained with Langmuir isotherm which is in good agreement with the equation:

$$\frac{C}{\theta} = \frac{1}{K} + C \qquad (8)$$

where C is inhibitor concentration and K is the equilibrium constant for the adsorption-desorption process. The surface coverage values, θ ($\theta = (\eta_{WL}/\%)/100$), for different concentrations of CNEO were used to explain the best adsorption isotherm. A plot of C/θ versus C (Figure 4) gives a straight line with an average correlation coefficient of 0.99 and a slope of nearly unity suggests that the adsorption of active organic molecules of CNEO obeys Langmuir adsorption isotherm.

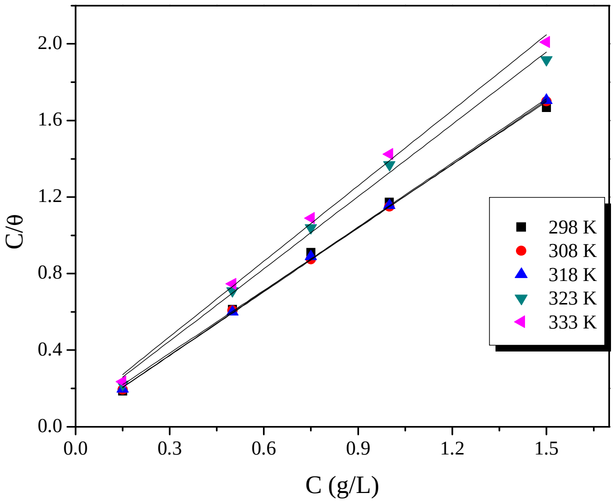

Figure 4: Langmuir adsorption plots of mild steel in 1.0 M HCl solution containing different concentrations of CNEO at different temperature

The Langmuir adsorption isotherm is based on the assumption that all adsorption sites are equivalent and the binding of particles occurs independently from nearby sites being occupied or not [56]. This indicates that the adsorbing species of CNEO occupies typical adsorption site at the metal/solution interface. Moreover it is not possible to discuss the adsorption behavior of plant extracts and essential oils as inhibitors in terms of thermodynamic parameters, such as the standard free energy of adsorption value because the molecular mass of the extract and oil components is not known. The same limitation has been noted by some authors [57,58].

Potentiodynamic Polarization Measurements

The polarization behavior of the mild steel in 1.0 M HCl solution in the presence and absence of *cymbopogon nardus* essential oil (CNEO) is shown in Fig. 5. The anodic and cathodic current potential curves were extrapolated to their intersection at the point where the corrosion current density (I_{corr}), the cathodic and anodic Tafel slopes (β_c and β_a), the corrosion potential (E_{corr}), and the inhibition efficiency were obtained from polarization measurements. As evident from results in Table 3, the I_{corr} value decreases from 1046.7to 113.4 $\mu A/cm^2$ in the presence of *cymbopogon nardus* essential oil (CNEO) as a consequence of an increase in the fraction of the electrode surface blocked by adsorption [59].

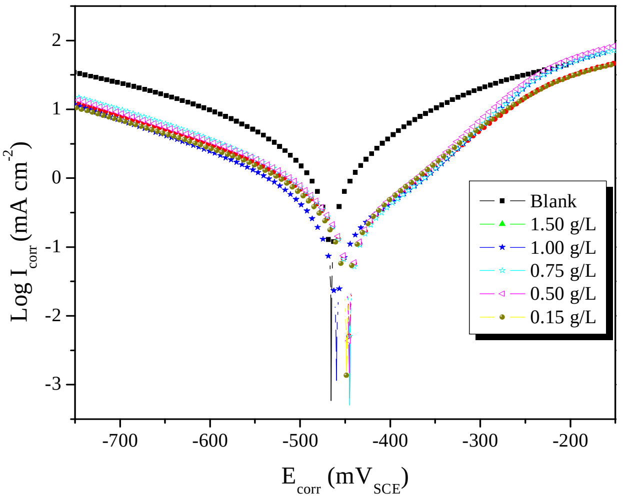

Figure 5: Potentiodynamic polarization curves for the mild steel in 1.0 M HCl in the absence and presence of different concentrations of CNEO at 298 K

Table 3: Electrochemical parameters for the mild steel determined from Tafel polarization

Inhibitor	Conc (g/L)	-E_{corr} (mV$_{SCE}$)	-β_c (mV/dec)	I_{corr} (µA cm^{-2})	η_{Tafel} (%)
1.0 M HCl	—	465.5	125	1046.7	—
CNEO	1.50	462.2	79.6	113.4	89.2
	1.00	459.7	73.8	119.8	88.5
	0.75	445.0	78.6	147.1	85.9
	0.50	445.6	76.7	153.5	85.3
	0.15	448.3	99.5	183.1	82.5

A change in the E_{corr} value is also noticed in the presence of CNEO. According to Ferreira et al. [60], (i) if the displacement in the E_{corr} value is greater than 85 mV, the inhibitor acts as a cathodic-or anodic-type inhibitor; (ii) if the displacement in the E_{corr} value is less than 85 mV, the inhibitor is considered a mixed-type inhibitor. In the present study, the maximum displacement in the E_{corr} value is 20.5 mV, which indicates that the studied inhibitor is a mixed-type inhibitor.

As evident in Fig. 5, the anodic reactions of steel electrode corrosion are inhibited with increasing CNEO concentration. Also, the addition of CNEO suppresses the anodic reactions to a lesser extent than the cathodic reactions. This result indicates that the addition of CNEO reduces the anodic dissolution and retards the hydrogen evolution reaction, which suggests that the CNEO acts as a mixed-type inhibitor.

Electrochemical impedance spectroscopy

The EIS of mild steel electrode in 1 M HCl solution in the absence and presence of CNEO are shown in Fig. 6. All the impedance spectra were measured at the corresponding open-circuit potentials.

As shown in Fig. 6, when CNEO is added to the corrosive solution, the Nyquist diagrams are larger than in the blank solution; this result accounts for the inhibitive effect of the CNEO molecules. The size of the impedance diagram increases as the concentration rises and consequently the protection efficiency increases. On the other hand, the inspection of the EIS data reveal that the impedance diagram obtained with 1.0 M HCl shows only one capacitive loop at high frequency (HF) values. The same trend (one capacitive loop) was also noticed for mild steel immersed in 1.0 M HCl containing different concentration of inhibitor (0.15 to 1.50 g/L). As usually indicated in the EIS study, the HF capacitive loop, is related to the charge transfer process of the metal corrosion and double layer behaviour. The above impedance diagrams (Nyquist) are not perfect semicircles from EIS theory in the frequency range with the centre under the real axis. This behaviour is characteristic for solid electrodes and usually referred to frequency dispersion which has been attributed to the inhomogeneities of the metal surfaces and mass transport processes [61]. Thus, in these situations pure double layer capacitors are better described by a transfer function with constant phase elements (CPE) to get a more accurate fit of experimental data set [61]. Its impedance is given by:

$$Z_{CPE} = A^{-1} (i\,\omega)^{-n} \quad (9)$$

where A is the CPE constant, ω is the angular frequency (in rad s^{-1}), i^2 =-1 is the imaginary number and n is a CPE exponent which can be used as a gauge of the heterogeneity or roughness of the surface [62]. Depending on the value of n, CPE can represent resistance (n= 0, A = R), capacitance (n=1, A = C), inductance (n = −1, A = L) or Warburg impedance (n = 0.5, A =W).

The impedance spectra were fitted by a simple Randles circuit (Fig. 7), which consists of R_s solution resistance, R_{ct} charge transfer resistance and CPE constant phase elements for the double layer. A constant phase element (CPE) is used instead of a pure capacitor to compensate for non-ideal capacitive response of the interface [63,64]. The charge transfer resistance is corresponding to the corrosion reaction at metal substrate/solution interface, whose value is a measure of electron transfer across the surface and is proportional to corrosion rate. Good fit is obtained (Fig. 8, representative example), meaning that the suggested equivalent circuit model (Fig. 7) could reasonably represent the charge transfer and metal/solution interface features related to the corrosion process of mild steel in acidic solution containing CNEO. The electrochemical impedance parameters obtained from fitting the recorded EIS data using the equivalent circuit of Fig. 7, are listed in Table 4.

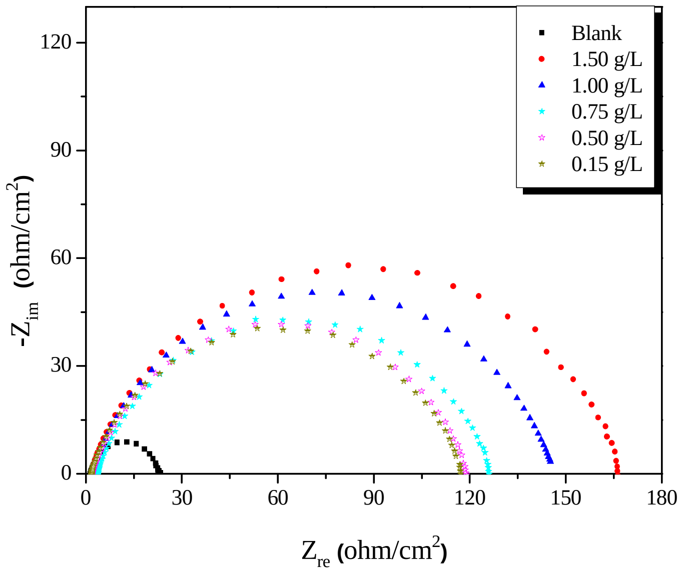

Figure 6: Nyquist plots for mild steel in 1.0 M HCl in the absence and presence of different concentrations of CNEO at 298K

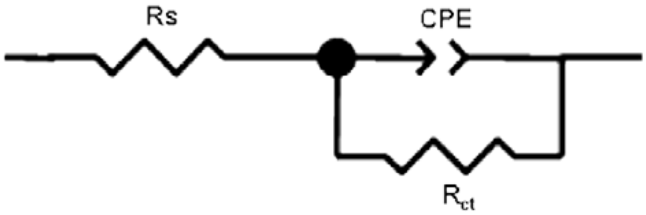

Figure 7: Electrical equivalent circuit used to fit the EIS data of the interface mild steel/1.0 M HCl solution without and with CNEO inhibitor

Table 4: Impedance parameters and inhibition efficiency values for mild steel in 1.0 M HCl without and with different concentrations of CNEO at 298 K

Conc	R_s (Ω cm^2)	R_{ct} (Ω cm^2)	n	C_{dl} (µF cm^{-2})	η_z (%)
1 .0 M HCl	2.00	22.75	0.89	155.2	—
1.50 g/L	1.70	165.33	0.78	60.4	86.3
1.00 g/L	1.87	143.67	0.78	90.3	84.1
0.75 g/L	3.46	123.09	0.78	92.3	81.5
0.50 g/L	2.06	117.15	0.79	101.4	80.4
0.15 g/L	1.56	116.04	0.79	108.7	80.3

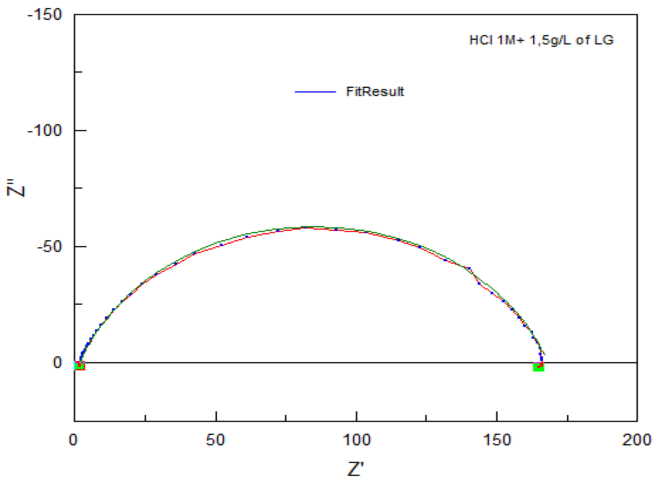

Figure 8: EIS Nyquist plots for mild steel/1.0 M HCl + 1.50 g/L CNEO interface: (….) experimental data; (—) calculated

From Table 4, it is clear that the addition of CNEO causes a significant increase in R_{ct} in the additive-free solution and diminishes the value of C_{dl}. The decrease in C_{dl} could be attributed to the adsorption of the inhibitor forming protective adsorption layers [65]. These findings indicate that, CNEO inhibit mild steel corrosion by adsorption. As, the impedance spectra show one capacitive loop, adsorption of CNEO occurs by simple surface coverage and CNEO act as a primary interface inhibitor [66]. In addition, the deviation parameter n has a tendency to decrease with the addition of inhibitor. The decrease in n may be connected with surface roughening which, due to the inhibitor molecules adsorbed on the metal surface, increase the heterogeneity [44]. The η(%) values obtained from the ac impedance technique are comparable and run parallel with those obtained from the weight loss measurements and the potentiodynamic polarization method.

CONCLUSION

The main conclusions drawn from these studies are weight loss, polarization studies, and impedance measurements which are in reasonably good agreement. Increasing the inhibitor concentration, the inhibition efficiency increases. At the concentration of 1.50 g/L, the *cymbopogon nardus* essential oil (CNEO) have shown maximum inhibition efficiencies of 90.0%. The inhibitory efficiencyincreases with the inhibitor concentration but decreases with the testing temperature. The adsorption of CNEO on the surface of mild steel in 1.0 M HCl follows a Langmuir adsorption isotherm. Tafel parameters give an idea this inhibitor is mixed-type in nature. EIS experimental data revealed frequency distribution of the capacitance, simulated as constant phase element. The impedance results indicate that the value of charge-transfer resistance (R_{ct}) increased and double layer capacitance (C_{dl}) decreased. This result can be attributed to the increase of thickness of electrical double layer.

REFERENCES

[1] H. H. Uhlig and R. W. Revie, Corrosion and corrosion control, *John Wiley, New York*, **1985**.
[2] D. A. Jones, Principles and Prevention of Corrosion, *Macmillan, New York*, **1992**.
[3] M. W. Ranney, Inhibitors-Manufacture and Technology, *Noyes Data Corp, New Jersey*, **1976**.
[4] H.A. Sorkhabi, D. Seifzadeh, M.G. Hosseini, *Corros. Sci*. **2008**, 50, 3363.
[5] A.H. Al Hamzi, H. Zarrok, A. Zarrouk, R. Salghi, B. Hammouti, S.S. Al-Deyab, M. Bouachrine, A. Amine, F. Guenoun, *Int. J. Electrochem*. Sci., **2013**, 8, 2586.
[6] A. Zarrouk**,** B. Hammouti, H. Zarrok, I. Warad, M. Bouachrine, *Der Pharm. Chem*., **2011**, 3, 263.
[7] D. Ben Hmamou, R. Salghi, A. Zarrouk, M. Messali, H. Zarrok, M. Errami, B. Hammouti, Lh. Bazzi , A. Chakir, *Der Pharm. Chem*., **2012**, 4, 1496.
[8] A. Ghazoui, N. Bencaht, S.S. Al-Deyab, A. Zarrouk, B. Hammouti, M. Ramdani, M. Guenbour, *Int. J. Electrochem. Sci*., **2013**, 8, 2272.
[9] A. Zarrouk, H. Zarrok, R. Salghi, N. Bouroumane, B. Hammouti, S.S. Al-Deyab, R. Touzani, *Int. J. Electrochem. S*ci., **2012**, 7, 10215.
[10] H. Bendaha, A. Zarrouk, A. Aouniti, B. Hammouti, S. El Kadiri, R. Salghi, R. Touzani, *Phys. Chem. N*ews, **2012**, 64, 95.
[11] A. Zarrouk, B. Hammouti, H. Zarrok, M. Bouachrine, K.F. Khaled, S.S. Al-Deyab, *Int. J. Electrochem. Sci*., **2012**, 6, 89.

[12] A. Ghazoui, R. Saddik, N. Benchat, M. Guenbour, B. Hammouti, S.S. Al-Deyab, A. Zarrouk, *Int. J. Electrochem. Sci*., **2012**, 7, 7080.
[13] H. Zarrok, K. Al Mamari, A. Zarrouk, R. Salghi, B. Hammouti, S. S. Al-Deyab, E. M. Essassi, F. Bentiss, H. Oudda, *Int. J. Electrochem. Sci*., **2012**, 7, 10338.
[14] H. Zarrok, A. Zarrouk, R. Salghi, Y. Ramli, B. Hammouti, M. Assouag, E. M. Essassi, H. Oudda and M. Taleb, *J. Chem. Pharm. Res*., **2012**, 4, 5048.
[15] A. Zarrouk, B. Hammouti, A. Dafali, F. Bentiss, *Ind. Eng. Chem. Res*. **2013**, 52, 2560.
[16] H. Zarrok, A. Zarrouk, R. Salghi, H. Oudda, B. Hammouti, M. Assouag, M. Taleb, M. Ebn Touhami, M. Bouachrine, S. Boukhris, *J. Chem. Pharm. Res*. **2012**, 4, 5056.
[17] H. Zarrok, H. Oudda, A. El Midaoui, A. Zarrouk, B. Hammouti, M. Ebn Touhami, A. Attayibat, S. Radi, R. Touzani, *Res. Chem. Intermed*. **2012**, 38, 2051.
[18] A. Ghazoui, A. Zarrouk, N. Bencaht, R. Salghi, M. Assouag, M. El Hezzat, A. Guenbour, B. Hammouti, *J. Chem. Pharm. Res*. **2014**, 6, 704.
[19] H. Zarrok, A. Zarrouk, R. Salghi, M. Ebn Touhami, H. Oudda, B. Hammouti, R. Touir, F. Bentiss, S.S. Al-Deyab, *Int. J. Electrochem. Sci*. **2013**, 8, 6014.
[20] A. Zarrouk, H. Zarrok, R. Salghi, R. Touir, B. Hammouti, N. Benchat, L.L. Afrine, H. Hannache, M. El Hezzat, M. Bouachrine, *J. Chem. Pharm. Res*. **2013**, 5, 1482.
[21] H. Zarrok, A. Zarrouk, R. Salghi, M. Assouag, B. Hammouti, H. Oudda, S. Boukhris, S.S. Al Deyab, I. Warad, *Der Pharm. Lett*. **2013**, 5, 43.
[22] D. Ben Hmamou, M.R. Aouad, R. Salghi, A. Zarrouk, M. Assouag, O. Benali, M. Messali , H. Zarrok, B. Hammouti, *J. Chem. Pharm. Res*. **2012**, 4, 3498.
[23] M. Belayachi, H. Serrar, H. Zarrok, A. El Assyry, A. Zarrouk, H. Oudda, S. Boukhris, B. Hammouti, Eno E. Ebenso, A. Geunbour, *Int. J. Electrochem. Sci*. **2015**, 10, 3010.
[24] H. Tayebi, H. Bourazmi, B. Himmi, A. El Assyry, Y. Ramli, A. Zarrouk, A. Geunbour, B. Hammouti, Eno E.Ebenso, *Der Pharm. Lett*. **2014**, 6(6), 20.
[25] H. Tayebi, H. Bourazmi, B. Himmi, A. El Assyry, Y. Ramli, A. Zarrouk, A. Geunbour, B. Hammouti, *Der Pharm. Chem*. **2014**, 6(5), 220.
[26] P. B. Raja, M. G. Sethuraman, *Mater. Lett*. **2008**, 62, 113.
[27] M. A. Ameer, A. M. Fekry, *Prog. Org. Coat*. **2011**, 71, 343.
[28] L. R. Chauhan, G. Gunasekaran, *Corros. Sci*. **2007**, 49, 1143.
[29] M. H. Hussin, M. J. Kassim, *Mater. Chem. Phys*. **2011**, 125, 461.
[30] A. Bouyanzer, L. Majidi, B. Hammouti, *Phys. Chem. News* **2007**, 37, 70.
[31] A. Chetouani, B. Hammouti, M. Benkaddour, *Pigment Resin Technol*. **2004**, 33, 26.
[32] M. Benabdellah, M. Benkaddour, B. Hammouti, M. Bendahhou, A. Aouniti, *Appl. Surf. Sci*. **2006**, 252, 6212.
[33] A. Bouyanzer, B. Hammouti, L. Majidi, *Mater. Lett*. **2006**, 60, 2840.
[34] M. Gong, F-Y. Mao, J-P. Wu, X-G. Zeng, *Corros. Prot*. **2006**, 27, 576.
[35] S. Rekkab, H. Zarrok, R. Salghi, A. Zarrouk**,** Lh. Bazzi, B. Hammouti, Z. Kabouche, R. Touzani, M. Zougagh, *J. Mater. Environ. Sci*., **2012**, 3, 613.
[36] J. Halambek, K. Berkovic´, J. Vorkapic´ -Furacˇ, *Corros. Sci*. **2010**, 52, 3978.
[37] D. Ben Hmamou, R. Salghi, A. Zarrouk, S.S. Al-Deyab, H. Zarrok, B. Hammouti, E. Errami, *Int. J. Electrochem. Sci*. **2012**, 7, 6234.
[38] I. Hamdani, E. El Ouariachi, O. Mokhtari, A. Salhi, A. Bouyanzer, A. Zarrouk, B. Hammouti, J. Costa, *Der Pharm. Lett*. **2015,** 7 (9), 109.
[39] N. Lotfi, F. Benhiba, N. Chahboun, H. Bourazmi, M. El Hezzat, A. H. Al Hamzi, H. Zarrok, A. Guenbour, M. Ouhssine, H. Oudda and A. Zarrouk, *Der Pharm. Lett*. **2015**, 7 (9), 1.
[40] I. Hamdani, E. El Ouariachi, O. Mokhtari, A. Salhi, N. Chahboun, B. ElMahi, A. Bouyanzer, A. Zarrouk, B. Hammouti and J. Costa, *Der Pharm. Chem*., **2015**, 7(8), 252.
[41] ASTM, G 31-72, American Society for Testing and Materials, Philadelphia, PA, **1990**.
[42] S.A Ali, A.M El-Shareef, R.F Al-Ghandi, M.T. Saeed, *Corros. Sci*. **2005**, 47, 2659.
[43] X. Li, S. Deng, H. Fu, G. Mu, *Corros. Sci*. **2009**, 51, 620.
[44] A. Popova, E. Sokolova, S. Raicheva, M. Christov, *Corros. Sci*. **2003**, 45, 33.
[45] A. Ostovari, S.M Hoseinieh, M. Peikari, S.R Shadizadeh, S.J. Hashemi, *Corros. Sci*. **2009**, 51, 1935.
[46] S. Martinez, I. Stern, *Appl. Surf. Sci*. **2002**, 199, 83.
[47] N.O Obi-Egbedi, I.B. Obot, *Corros. Sci*. **2011**, 53, 263.
[48] A.S Fouda, F.E Heakal, M.S. Radwan, *J. Appl. Electrochem*. **2009**, 39, 391.
[49] L.R Chauhan, G. Gunasekaran, *Corros. Sci*. **2007**, 49,1143.
[50] A.Y Musa, A.A.H Kadheem, A.B Mohamad, A.R Daud, M.S Takriff, S.K. Kamarudin, *Corros. Sci*. **2009**, 51, 2393.
[51] A. Ostovari, S.M Hoseinieh, M. Peikari, S.R Shadizadeh, S.J. Hashemi, *Corros. Sci*. **2009**, 51, 1935.
[52] J.O'M. Bochris, A.K.N. Reddy, Modern Electrochemistry, *Plenum Press*, New York, **1977**, 2, 1267.

[53] G.N Mu, X. Li, F. Li, *Mater. Chem. Phys*. **2004**, 86, 59.
[54] N.O Obi-Egbedi, I.B. Obot, *Arab. J. Chem*. **2012**, 5, 121.
[55] X. Wu, H. Ma, S. Chen, Z. Xu, A. Sui, *J. Electrochem. Soc*. **1999**, 146, 1847.
[56] K.F Khaled, N. Hackerman, *Electrochim. Acta* **2003**, 48, 2715.
[57] R. Kanojia, G. Singh, *Surf. Eng*. **2005**, 21, 180.
[58] E.A. Noor, *Int. J. Electrochem. Sci*. **2007**, 2, 996.
[59] F. Bentiss, M. Traisnel, H. Vezin, H.F. Hildebrand, M. Lagrenée, *Corros. Sci.* **2004**, 46, 2781.
[60] E.S. Ferreira, C. Giancomelli, F.C. Giacomelli, A. Spinelli, *Mater. Chem. Phys.* **2004**, 129.
[61] I.D. Raistrick, D.R. Franceschetti, J.R. Macdonald, in: E. Barsoukov, J.R. Macdonald (Eds.), Impedance Spectroscopy: Theory, Experimental and Applications, second ed., *John Wiley & Sons, New Jersey*, **2005**.
[62] J.W. Schultze, K. Wippermann, *Electrochim. Acta* **1987**, 32, 823
[63] C.H. Hsu, F. Mansfeld, *Corrosion* **2001**, 57, 747.
[64] D.A. Lopez, S.N. Simison, S.R. deSanchez, *Electrochim. Acta* **2003**, 48, 845.
[65] E. McCafferty, N. Hackerman, *J. Electrochem. Soc*. **1972**, 119, 146.
[66] H. Fischer, *Werkst. Korros*. **1972**, 23, 445.